2008 IEEE International Conference on
Robotics and Automation
Pasadena, CA, USA, May 19-23, 2008

Design of an Omnidirectional Mobile Robot for Rough Terrain

Martin Udengaard and Karl Iagnemma

Massachusetts Institute of Technology
Cambridge, MA 02139 USA
{mru, kdi}@mit.edu

***Abstract*—An omnidirectional mobile robot is able, kinematically, to move in any planar direction regardless of current pose. To date, nearly all designs and analyses of omnidirectional robots have considered the case of motion on flat, smooth terrain. This paper presents design constraints and guidelines for designing an omnidirectional mobile robot propelled by active split offset casters to be driven in rough terrain. Geometric constraints on wheel and linkage sizes are presented. The effects of terrain roughness and loss of wheel contact are analyzed. The vehicle design is optimized for kinematic isotropy, ability to maintain ground contact, traversable obstacle height, and maximum traversable distance over four diverse terrain types. The results are contrasted with a baseline design.**

Index Terms-Omnidirectional vehicle, rough terrain, isotropy, mobile robots, design

I. Introduction

Mobile robots are finding increasing use in military [1], disaster recovery [2], and exploration applications [3]. These applications frequently require operation in rough, unstructured terrain. Currently, most mobile robots designed for these applications are tracked or Ackermann-steered wheeled vehicles. Methods for controlling these types of robots in both smooth and rough terrain have been well studied [4-7]. While these robots types can perform well in many scenarios, navigation in cluttered, rocky, or obstacle-dense urban environments can be difficult or impossible. This is partly due to the fact that traditional tracked and wheeled robots must reorient to perform some maneuvers, such as lateral displacement. Omnidirectional mobile robots could potentially navigate faster and more robustly through cluttered urban environments and over rough terrain, due to their ability to track near-arbitrary motion profiles.

An omnidirectional mobile robot is able, kinematically, to move in any planar direction regardless of current pose. Previous researchers have proposed and developed omnidirectional mobile robots employing a wide variety of wheel types including roller [8,9], Mecanum [10,11], and spherical wheels [12,13].

An omnidirectional mobile robot driven by active split offset casters (ASOC) modules was initially proposed in [14] for use in structured, indoor environments. ASOC modules employ conventional wheel designs that do not use small rollers or frictional drives, and are thus potentially suitable for use in dirty, outdoor environments. They also can be designed with little constraint on wheel diameter and width, and thus can potentially tolerate large loads with low ground pressure. Finally, ASOC modules can be integrated with suspension systems that allow for traversal of uneven terrain [15]. Therefore ASOC-driven omnidirectional mobile robots hold promise for use in rough, unstructured environments.

In this paper, design considerations for an ASOC-driven omnidirectional mobile robot for operation in rough terrain are presented. The design parameters examined include the number of ASOC modules, kinematic parameters of the ASOC, module location, and wheel geometry. The parameters are optimized for isotropy, ability to maintain ground contact, obstacle height, and maximum traversable distance over four diverse terrain types. It is shown that an optimized design will outperform a baseline design based on engineering estimates.

II. Active Split Offset Caster Description

ASOC drive modules possess the ability to achieve omnidirectional motion via a driven wheel pair. Figure 1 shows the ASOC module geometry considered in this study. The assembly consists of a split wheel pair, a connecting axle, and an offset link connecting the wheel pair to the mobile robot body. Each wheel is independently driven about the axis θ. The axle connecting the wheel pair can pivot about the axis β. This joint can be passive or active, and allows the wheel pair to adapt to terrain unevenness, thereby increasing terrain contact for each wheel even during travel on rough terrain. The wheel pair/axle assembly rotates passively about axis α. This axis connects the ASOC module to a robot body or a passive or active suspension element. L_{offset} is the distance between the axis α and the axis θ. L_{split} is the distance between the wheels.

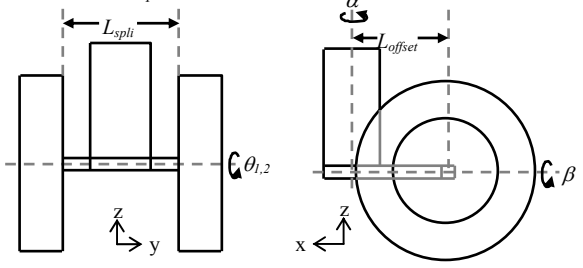

Figure 1. Side and front views of an active split offset caster module

Manuscript received Sep 14, 2007. This work was sponsored by the U. S. Army Research Office under grant number W911NF-05-1-0166.

By independently controlling each wheel's velocity, an ASOC module can produce arbitrary (planar) translational velocities at a point along its α axis. Two or more ASOC modules attached to a rigid robot body can thus produce arbitrary translational and rotational robot velocities. Therefore, an ASOC-driven omnidirectional robot must minimally employ two ASOC modules, and can employ more to meet other design requirements related to thrust, ground pressure, tip-over stability, etc. Note that passive or active casters can also be used to augment ASOC modules to meet these requirements. A kinematic analysis of ASOC modules is presented in [14].

III. Design Objectives

The design considered in this paper is a man-portable, battery powered mobile robot with a maximum enclosed envelope of one cubic meter and mass of 65 kg. The primary design objective is to maximize traversable distance over a range of outdoor terrain types while maintaining a high level of mobility (quantified by system kinematic isotropy, the ability of an ASOC module to maintain ground contact, and traversable obstacle height). The robot must operate under its own power, and therefore should maximize mass efficiency to increase its battery payload. It should also minimize power loss from motion resistance in deformable terrain. Factors influencing the design space include wheel width, wheel radius, ASOC split and offset lengths, and the number and relative location of ASOC modules. Geometric constraints that bound the allowable design space must also be considered.

Figure 2 shows an illustration of an omnidirectional mobile robot driven by four ASOC modules. This is a representative configuration that will be considered in this work; however the analysis is general and applies to robots with N ASOC modules.

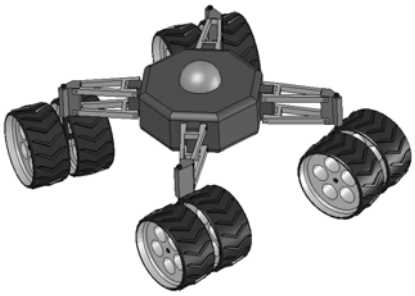

Figure 2. Illustration of an ASOC-driven omnidirectional mobile robot. This robot has four ASOC modules spaced at 90° intervals.

IV. Geometric Constraints

The unique geometry of the ASOC and the large range of motion of each module constrains the size of some components. Potentially, a control algorithm could utilize the robot's redundancy to relax these constraints (by ensuring that wheel pairs are never directly oriented towards each other, for example). However, such an algorithm would likely reduce overall system mobility. Therefore, a geometric analysis of the ASOC module workspace and maximum pivot angle range of motion is presented.

4.1 ASOC Workspace Analysis

The maximum allowable wheel size that does not risk ASOC interference can be calculated by simple geometric analysis of the module workspace. As seen in Figure 3, the minimum distance between adjacent ASOC axes, d_a, must be at least twice the maximum radius of the ASOC module workspace, $r_{workspace}$. This radius is the distance from the vertical axis to the most distal point on the wheel:

$$r_{workspace} = \sqrt{\left(L_{offset} + r_{wheel}\right)^2 + \left(0.5L_{split} + w_{wheel}\right)^2}\,, \qquad (1)$$

where r_{wheel} and w_{wheel} are the wheel radius and width.

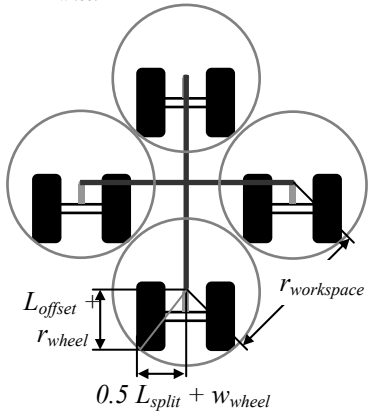

Figure 3. The circles represent the boundaries of the ASOC module workspace. To avoid ASOC interference, they should not intersect.

4.2 Maximum Pivot Angle Analysis

In rough terrain, the passive axis β (see Figure 1) allows the ASOC wheels to conform to terrain unevenness. A potential limiting factor of β axis travel is wheel-shaft interference (see Figure 4).

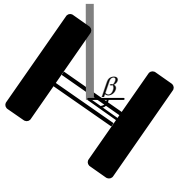

Figure 4. Rear view of ASOC with wheel-shaft interference.

The maximum allowable rotation angle of β can be calculated as the angle at which the inner rim of the wheel intersects with the vertical shaft that connects the module to the robot body. This occurs when

$$0.5L_{split}\cos\beta = r_{wheel.effective}\sin\beta\,, \qquad (2)$$

where $r_{wheel.effective}$ is the vertical distance from the center of the wheel to the section of the rim that can intersect the shaft, as shown in Figure 5.

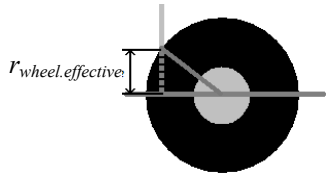

Figure 5. Depiction of $r_{wheel.effective}$.

The value of $r_{wheel.effective} = \sqrt{r_{wheel}^2 - L_{offset}^2}$. Note that when $L_{offset} > r_{wheel}$, the shaft and wheel cannot interfere. However, such a configuration would potentially cause the ASOC axis to collide with obstacles before they contact the wheels, which is undesirable. In a nominal configuration, the maximum value of β is given as

$$\beta_{\max} = \tan^{-1}\left(0.5L_{split} \Big/ \sqrt{r_{wheel}^2 - L_{offset}^2}\right). \quad (3)$$

V. Isotropy Analysis

Path following in rough terrain may require a robot to quickly change its direction of travel. All omnidirectional mobile robots are kinematically able to instantaneously travel in any planar direction. However, while some omnidirectional mobile robots exhibit preferred directions of travel, others exhibit equal mobility in all directions. Hence, isotropy is used to quantify the system's omnidirectional mobility.

Kinematic isotropy is defined as the condition in which a robot possesses a constant input velocity/output velocity ratio for all possible output velocity directions [16]. An isotropy metric is a measure of how near a robot is to the isotropy condition, and increases from 0.0 for a singular configuration (i.e. purely anisotropic, or non-omnidirectional) to 1.0 for kinematic isotropy. Ideally, an omnidirectional robot should possess a metric value of 1.0 for all joint space configurations, and thus not have a preferred direction of travel. This simplifies path planning and navigation by eliminating the effect of robot orientation on movement capability. The output directions considered in this study are two planar translations in the robot body frame, and rotation about the robot body frame z axis.

The isotropy metric for a given robot configuration can be computed as the ratio of the smallest to largest eigenvalues of the Jacobian matrix relating the driving module velocities to the robot body velocities [16]. The isotropy metric can be averaged over the entire configuration space (in this case, the rotation angles between each ASOC and the body, α) to yield an average measure of performance that could be used to compare candidate omnidirectional mobile robot designs.

5.1 Effect of ASOC Kinematic Parameters on Isotropy

To analyze the effects of ASOC module kinematic parameters on isotropy, L_{offset} and L_{split} were varied over a range of values that represent a practical omnidirectional robot design space. Note that in Figure 6, L_{offset} and L_{split} are normalized by the robot body length, defined as the length of the longest side of the robot body.

An iso-height exists at an isotropy value of 1.0. This iso-height occurs at $L_{split} / L_{offset} = 2.0$. The sensitivity of isotropy to perturbations in L_{split} and L_{offset} is relatively high; a 10% change in L_{split} or L_{offset} decreases the isotropy metric value by up to 45% for small ASOC module sizes.

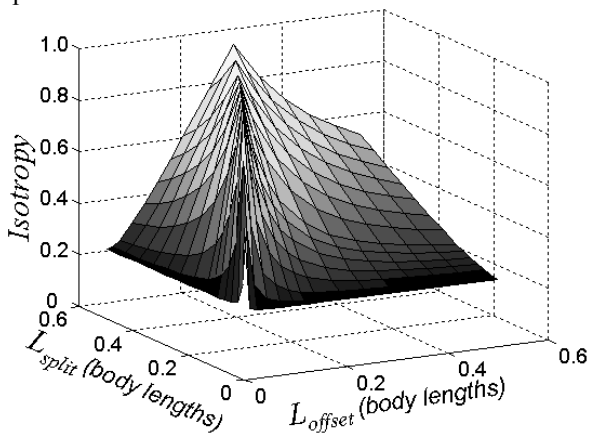

Figure 6. Average isotropy for a four ASOC omnidirectional robot.

Figure 7 is a plot of isotropy values over a range of L_{split} / L_{offset} ratios. From this figure it can be seen that there exists a single isotropy value for each L_{split} / L_{offset} ratio, indicating that isotropy is not an independent function of both L_{split} and L_{offset}. This is a useful insight for omnidirectional robot design. This also explains the sensitivity of isotropy to changes in L_{split} and L_{offset} for small ASOC modules sizes, since a unit change in L_{split} or L_{offset} results in a relatively large change in L_{split} / L_{offset} for small parameter values.

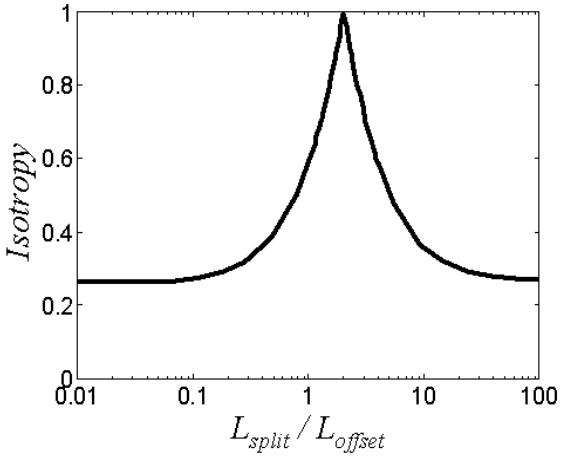

Figure 7. Average isotropy for omnidirectional robot driven by four ASOC modules as a function of L_{split} / L_{offset}.

5.2 Effect of ASOC Module Location on Isotropy

The relative location of ASOC modules also affects isotropy. A plot of isotropy as a function of relative ASOC angular location is presented in Figure 8. Note that a vehicle with three modules, shown in Figure 9, was chosen for analysis so that the results can be visually presented in two dimensions. Each ASOC had a L_{split} / L_{offset} ratio of 2.0. ASOC interference was neglected.

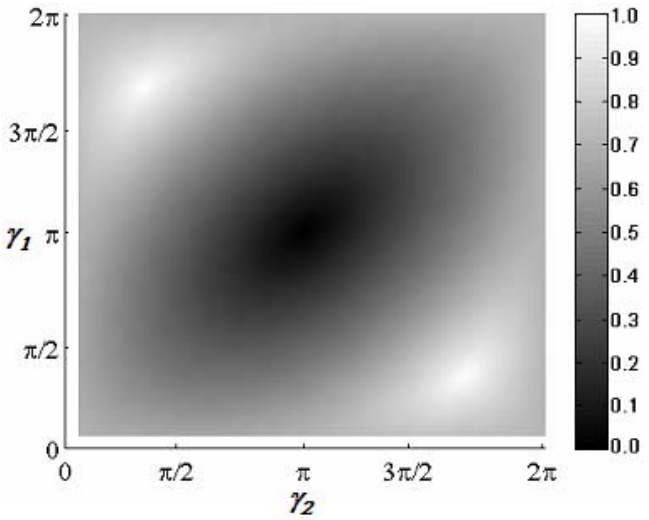

Figure 8. Isotropy as a function of ASOC module relative location

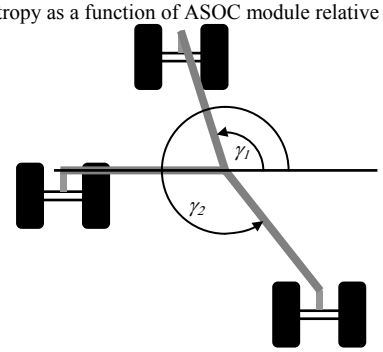

Figure 9. Top view of representative vehicle for ASOC location analysis

It can be shown that maximum isotropy values (1.0) are obtained when the ASOC modules are evenly spaced. The value drops to 0 for the degenerate case where all ASOC modules coincide. A similar phenomenon is observed for robots with any number of ASOC modules. Thus to maximize isotropy, ASOC modules should be equally spaced.

5.3 Effect of Loss of Wheel Contact on Isotropy

When traversing rough terrain, loss of contact may occur between the wheels and the ground. In this case, system mobility will be decreased. An analysis of the isotropy of robots without full ground contact is presented in Table I. For comparison, robots with two, three, and four ASOC modules are examined. Each ASOC is allowed to possess full, partial (one wheel on the ground), or no ground contact.

TABLE I
EFFECT OF LOSS OF WHEEL CONTACT ON ISOTROPY

Total # ASOCs	# no contact ASOCs	# partial contact ASOCs				
		0	1	2	3	4
2	0	1.000	0.464	0.000	N/A	N/A
3	0	1.000	0.706	0.504	0.270	N/A
	1	0.577	0.367	0.000	N/A	N/A
4	0	1.000	0.791	0.656	0.544	0.399
	1	0.707	0.574	0.482	0.259	N/A
	2	0.414	0.265	0.000	N/A	N/A

As expected, loss of wheel contact causes reduced isotropy due to a loss of full controllability of the ASOC modules. It can be observed that a four ASOC robot with one module that has completely lost terrain contact does not perform as well as a three ASOC vehicle in full contact. This is due to the fact that the three ASOC robot has evenly spaced ASOC modules. Also, given an identical number of wheels without terrain contact (e.g., 0 no contact and 2 partial contact vs. 1 no contact and 0 partial contact), a robot generally has higher isotropy when terrain contact is lost on the same ASOC, since more modules remain fully engaged with the ground. The isotropy loss from partial contact ASOC modules reinforces the importance of the axle pivot.

Finally, a vehicle with a greater number of ASOCs will have a relatively smaller drop in isotropy for each lost wheel contact, but may have increased difficulty keeping all wheels in contact with the ground due to increased suspension complexity. Additional modules also add mass while decreasing the allowable wheel size (see Section IV) and available battery mass.

5.4 Effect of Terrain Roughness on Isotropy

Isotropy of an omnidirectional robot can also be affected by terrain roughness. Variation in terrain inclination among ASOC modules, or among ASOC module wheel pairs, causes a change in the effective value of L_{split} with respect to the body frame, which yields a change in L_{split} / L_{offset} and thus a change in isotropy (see Figure 10). As mentioned in Section II, axis β allows ASOC wheels to maintain contact during travel on uneven terrain.

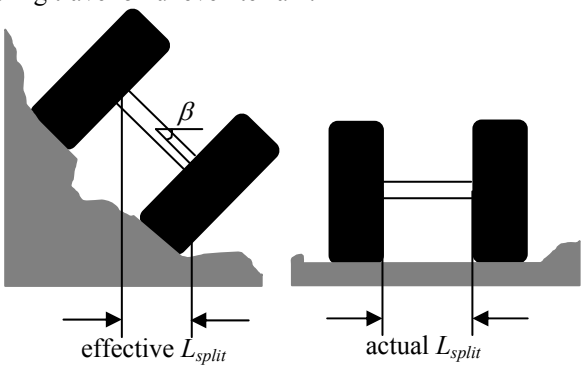

Figure 10. ASOC module on flat and rough terrain. Rough terrain can cause the module to pivot about the β axis, decreasing the effective L_{split}.

In theory, L_{split} could be modified as a function of terrain inclination via an active, extensible axle to cause the effective L_{split} / L_{offset} ratio to always be near 2.0, thus yielding good isotropy characteristics on rough terrain. In practice, however, such a design would be cumbersome and impractical. Thus it is useful to examine the effects of terrain inclination on robot isotropy.

In Figure 11, a contour plot is presented of the average isotropy over a range of static robot configurations and terrain angles. It can be seen that the L_{split} / L_{offset} ratio with the largest isotropy value increases with the maximum

terrain angle. Larger angles decrease the effective ratio and thus the "true" ratio must therefore increase. Maximum average isotropy also decreases slightly with increasing terrain angle. Table II summarizes these findings.

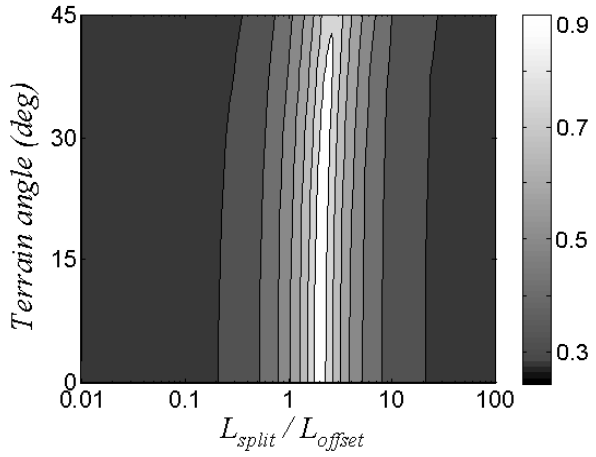

Figure 11. Mean isotropy as a function of L_{split} / L_{offset} and terrain angle.

TABLE II
EFFECT OF TERRAIN ON ISOTROPY AND IDEAL SPLIT/OFFSET RATIO

Terrain angle	Max isotropy	Optimum L_{split} / L_{offset} ratio
0° (flat)	1.000	2.00
0-15°	0.987	2.05
0-30°	0.950	2.27
0-45°	0.895	2.70

VI. DESIGN OPTIMIZATION

A design optimization was performed using the objectives outlined in Section III and constraints outlined in Section IV. The optimization varies the number of ASOC modules, L_{split}, L_{offset}, r_{wheel}, and w_{wheel} to maximize the objective function, J, computed as the sum of the normalized mobility parameters:

$$J = \frac{K}{K^*} + \frac{\beta_{\max}}{\beta_{\max}^*} + \frac{h}{h^*} + \frac{d_{\max}}{d_{\max}^*}, \quad (4)$$

where K is the kinematic isotropy, β_{max} is the maximum β axis pivot, h is the maximum obstacle height, and d_{max} is the maximum traversable distance. The star superscript refers to the maximum value of each parameter in the design space. The optimization consisted of a full factorial analysis over the design space to maximize the value of the objective function.

In this analysis, maximum pivot angle and kinematic isotropy are calculated as described in Sections IV and V. The maximum obstacle height is assumed to be a linear function of the wheel radius.

The optimization algorithm estimates maximum traversable distance by first determining the maximum available onboard energy. For the purposes of this study, it is assumed that the vehicle is powered by batteries with an energy density ρ_{energy} of 576 kJ/kg (similar to that of lithium-ion batteries). The maximum allowable onboard battery mass, $M_{battery}$, is the difference between the non-battery mass (i.e., wheels, structural components, electronics, etc.) and the predetermined total allowable mass. In this study, the mission specific total available mass limit was 65 kg. Wheel and ASOC masses are computed as a function of their sizes.

The energy consumed during forward travel is then estimated using an expansion of a semi-empirical formulation for compaction resistance on deformable terrain [17].

$$CR = \frac{n_{wheels}}{(3-n)^{\left(\frac{2n+2}{2n+1}\right)}(n+1)w_{wheel}^{\left(\frac{1}{2n+1}\right)}\left(k_c/w_{wheel}+k_\phi\right)^{\left(\frac{1}{2n+1}\right)}}\left[\frac{3\frac{Mg}{n_{wheels}}}{\sqrt{r_{wheel}}}\right]^{\left(\frac{2n+2}{2n+1}\right)} \quad (5)$$

In the equation above, CR is the compaction resistance (N), M is the total vehicle mass (kg), n_{wheels} is the number of wheels, and n, k_c, and k_ϕ are terrain physical constants (shown in Table III [18,19]). Note that this estimate is for straight driving and does not take into account other resistive forces (such as bulldozing forces) or energy used by other onboard devices.

TABLE III
TERRAIN PARAMETERS

Terrain type	n	k_c (kPa/m^{n-1})	k_ϕ (kPa/m^n)
Dry sand	1.1	0.9	1523.4
Sandy loam	0.7	5.3	1515.0
Clayey soil	0.5	13.2	692.2
Snow	1.6	4.4	196.7

The maximum traversable distance is approximated as $d_{max} = M_{battery}\rho_{energy}/CR$. Since the optimization compares similar systems, motor and drivetrain efficiencies are assumed identical for all candidate designs and therefore are not considered in the calculations.

VII. DESIGN OPTIMIZATION RESULTS

Table IV compares the values of the mobility parameters of robots with three, four, and five ASOC modules. The robots were optimized for sandy loam. Results are presented relative to the robot with three ASOC modules.

TABLE IV
EFFECT OF NUMBER OF ASOCS ON MOBILITY PARAMETERS

# ASOCs	K	β_{max}	h	d_{max}
3	0%	0%	0%	0%
4	0%	0%	0%	-41.4%
5	-2.2%	16.2%	-60.9%	-52.9%

A robot with four ASOC modules has similar values of kinematic isotropy (K), maximum β axis pivot angle (β_{max}), and maximum traversable obstacle height (h) as a three ASOC robot, however, adding the fourth module decreases available battery mass, and therefore decreases maximum traversable distance (d_{max}). A fifth ASOC module requires

smaller wheels, resulting in lower maximum traversable obstacle height, but higher maximum β axis pivot angle.

Table V shows the values of the geometric parameters for a three ASOC robot derived using the optimization algorithm and geometric constraints described above. Optimizations were calculated over the four terrain types shown in Table III, assuming randomized rough terrain with an angle range of 0-30°. Table VI shows the change in mobility parameter values for optimized designs compared to a baseline design with parameters determined by engineering judgment (L_{offset}=0.15 m, L_{split}=0.20 m, r_{wheel}=0.15 m, w_{wheel}= 0.03 m).

TABLE V
GEOMETRIC PARAMETERS FROM OPTIMIZATION

Terrain type	L_{offset} (m)	L_{split} (m)	r_{wheel} (m)	w_{wheel} (m)
Dry sand	0.144	0.325	0.148	0.090
Sandy loam	0.144	0.325	0.148	0.112
Clayey soil	0.134	0.306	0.139	0.133
Snow	0.144	0.325	0.148	0.054

TABLE VI
MOBILITY PARAMETER INCREASES FROM OPTIMIZATION

Terrain type	K	β_{max}	H	d_{max}
Dry sand	13.2%	85.2%	-1.4%	18.1%
Sandy loam	13.2%	85.2%	-1.4%	29.5%
Clayey soil	12.8%	82.8%	-7.4%	31.9%
Snow	13.2%	85.2%	-1.4%	3.3%

Note that the geometric parameter sets for relatively rigid terrains (i.e. sandy loam and clayey soil) had similar values. This implies that the robot could be adjusted to go from one surface to another by installing tires with a different width and changing the battery weight.

In all cases, the offset lengths were slightly smaller than the wheel radii, which yielded large allowable β tilt angles. The split offset ratios were all near 2.27:1, maximizing isotropy for the given terrain roughness range.

As presented, the optimizations for the relatively deformable terrains (i.e. dry sand and snow) resulted in wheels with larger radii, but narrower widths compared to those optimized for relatively rigid terrains. The large radii lead to decreased ground pressure and compaction resistance, while the thinner widths lead to decreased wheel weight. One could also minimize ground pressure by choosing a wider wheel, but for a given a depth of sinkage, a tall, narrow wheel has significantly less compaction resistance than a short, wide one. For the relatively rigid terrains, a wider wheel was preferred as it allowed a greater amount of onboard battery mass, thus increasing maximum traversable distance.

VIII. CONCLUSIONS

In this paper, numerous design considerations for omnidirectional mobile robots were presented. An optimization algorithm was implemented to derive values for ASOC module and wheel geometries. For illustration, a man portable robot was designed, but the geometric constraints and the optimization algorithm are scalable and can be applied to robots of any size. It was shown that the designs suggested by the optimization have increased performance when compared to a non-optimized design. Through deliberate ASOC geometric parameter selection, it was possible to increase estimated traversable distance versus a baseline design.

REFERENCES

[1] Fish, S., "UGV's in Future Combat Systems," *Proc of SPIE*, v 5422, *Unmanned Ground Vehicle Technology VI*, pp. 288-291, Apr 2004.

[2] Blitch, J., "Artificial Intelligence Technologies for Robot Assisted Urban Search and Rescue," *Expert Systems with Applications*, 1996.

[3] Erickson, J., "Living the Dream: An Overview of the Mars Exploration Project," *IEEE Robotics and Automation Magazine*, v 13, n 2, pp. 12-18, Jun 2006.

[4] Cheng, J., Gao, L., Wang, H., "Steering Analysis of Tracked Vehicles Based on Skid Condition," *Chinese Journal of Mechanical Engineering*, v 42, pp. 192-195, May 2006.

[5] Lindemann, R., Bickler, D., Harrington, B., Ortiz, G., Voorhees, C., "Mars Exploration Rover Mobility Development - Mechanical Mobility Hardware Design, Development, and Testing ," *IEEE Robotics and Automation Magazine*, v 13, n 2, pp. 19-26, Jun 2006.

[6] Ishigami, G., Miwa, A., Yoshida, K., "Steering Trajectory Analysis of Planetary Exploration Rovers Based on All-Wheel Dynamics Model," *Proc of the 8th Intl Symposium on Artificial Intelligence, Robotics and Automation in Space*, pp. 121-128, 2005.

[7] Iagnemma, K. and Dubowsky, S., *Mobile Robots in Rough Terrain: Estimation, Motion Planning, and Control with Application to Planetary Rovers*, Vol. 12, Springer, 2004.

[8] Fujisawa, S., Ohkubo, K., Yoshida, T., Satonaka, N., Shidama, Y., and Yamaura, H., "Improved Moving Properties of an Omnidirectional Vehicle Using Stepping Motor", *Proc of the 36th Conf on Decision & Control*. San Diego, California, pp.3654-7, 1997.

[9] Williams, R., Carter, B., Gallina, P., and Rosati, G., "Wheeled Omni-directional Robot Dynamics Including Slip," *Proc of 2002 ASME Design Engineering Technical Conferences,* Sep 2002.

[10] Muir, P., and Neuman, C., "Kinematic Modeling for Feedback Control of an Omnidirectional Wheeled Mobile Robot," *Proc. of 1987 IEEE Int. Conf. on Robotics and Automation,* 1987

[11] Bradley A., Miller, S., Creary, G., Miller, N., Begley, M., Misch, N., "Mobius, an Omnidirectional Robot Utilizing Mecanum Wheels and Fuzzy Logic Control," *Proc of the 28th Annual AAS Rocky Mountain Guidance and Control Conferences*, pp. 251-266, 2005.

[12] Ferriere L., Raucent B., "ROLLMOBS, a New Universal Wheel Concept," *Proc of 1998 IEEE ICRA,* pp. 1877-82, May 1998.

[13] West, A.M., and Asada, H., "Design of Ball Wheel Mechanisms for Omnidirectional Vehicles with Full Mobility and Invariant Kinematics," *ASME Journal of Mechanical Design,* 117, 1995.

[14] Yu, H., Dubowsky, S., and Skwersky, A., "Omni-directional Mobility Using Active Split Offset Castors." *Proc of the 26th ASME Biennial Mechanisms and Robotics Conf*, Sep 2000.

[15] Spenko, M., Yu, H., and Dubowsky, S., "Analysis and Design of an Omnidirectional Platform for Operation on Non-Ideal Floors," *Proc of IEEE Intl Conf on Robotics and Automation*, May 2002.

[16] Park, T., Lee, J., Yi, B., Kim, W., You, B., "Optimal Design and Actuator Sizing of Redundantly Actuated Omni-directional Mobile Robots," *IEEE ICRA,* pp.732-7, 2002.

[17] Bekker G. Theory of land locomotion, the mechanics of vehicle mobility. Ann Arbor: The University of Michigan Press; 1956.

[18] Yong R, Fattah E, Skiadas N. Vehicle traction mechanics. Amsterdam: Elsevier Science Publishers; 1984.

[19] Wong J. Terramechanics and offroad vehicles. Amsterdam: Elsevier Science Publishers; 1989.